

Search for the decays $J/\psi \rightarrow \gamma\rho\phi$ and $J/\psi \rightarrow \gamma\rho\omega$

M. Ablikim¹, J. Z. Bai¹, Y. Ban¹², X. Cai¹, H. F. Chen¹⁷, H. S. Chen¹, H. X. Chen¹, J. C. Chen¹, Jin Chen¹, Y. B. Chen¹, Y. P. Chu¹, Y. S. Dai¹⁹, L. Y. Diao⁹, Z. Y. Deng¹, Q. F. Dong¹⁵, S. X. Du¹, J. Fang¹, S. S. Fang^{1a}, C. D. Fu¹⁵, C. S. Gao¹, Y. N. Gao¹⁵, S. D. Gu¹, Y. T. Gu⁴, Y. N. Guo¹, Z. J. Guo^{16b}, F. A. Harris¹⁶, K. L. He¹, M. He¹³, Y. K. Heng¹, J. Hou¹¹, H. M. Hu¹, J. H. Hu³, T. Hu¹, G. S. Huang^{1c}, X. T. Huang¹³, X. B. Ji¹, X. S. Jiang¹, X. Y. Jiang⁵, J. B. Jiao¹³, D. P. Jin¹, S. Jin¹, Y. F. Lai¹, G. Li^{1d}, H. B. Li¹, J. Li¹, R. Y. Li¹, S. M. Li¹, W. D. Li¹, W. G. Li¹, X. L. Li¹, X. N. Li¹, X. Q. Li¹¹, Y. F. Liang¹⁴, H. B. Liao¹, B. J. Liu¹, C. X. Liu¹, F. Liu⁶, Fang Liu¹, H. H. Liu¹, H. M. Liu¹, J. Liu^{12e}, J. B. Liu¹, J. P. Liu¹⁸, Jian Liu¹, Q. Liu¹⁶, R. G. Liu¹, Z. A. Liu¹, Y. C. Lou⁵, F. Lu¹, G. R. Lu⁵, J. G. Lu¹, C. L. Luo¹⁰, F. C. Ma⁹, H. L. Ma², L. L. Ma^{1f}, Q. M. Ma¹, Z. P. Mao¹, X. H. Mo¹, J. Nie¹, S. L. Olsen¹⁶, R. G. Ping¹, N. D. Qi¹, H. Qin¹, J. F. Qiu¹, Z. Y. Ren¹, G. Rong¹, X. D. Ruan⁴, L. Y. Shan¹, L. Shang¹, C. P. Shen¹⁶, D. L. Shen¹, X. Y. Shen¹, H. Y. Sheng¹, H. S. Sun¹, S. S. Sun¹, Y. Z. Sun¹, Z. J. Sun¹, X. Tang¹, G. L. Tong¹, G. S. Varner¹⁶, D. Y. Wang^{1g}, L. Wang¹, L. L. Wang¹, L. S. Wang¹, M. Wang¹, P. Wang¹, P. L. Wang¹, Y. F. Wang¹, Z. Wang¹, Z. Y. Wang¹, Zheng Wang¹, C. L. Wei¹, D. H. Wei¹, Y. Weng¹, N. Wu¹, X. M. Xia¹, X. X. Xie¹, G. F. Xu¹, X. P. Xu⁶, Y. Xu¹¹, M. L. Yan¹⁷, H. X. Yang¹, Y. X. Yang³, M. H. Ye², Y. X. Ye¹⁷, G. W. Yu¹, C. Z. Yuan¹, Y. Yuan¹, S. L. Zang¹, Y. Zeng⁷, B. X. Zhang¹, B. Y. Zhang¹, C. C. Zhang¹, D. H. Zhang¹, H. Q. Zhang¹, H. Y. Zhang¹, J. W. Zhang¹, J. Y. Zhang¹, S. H. Zhang¹, X. Y. Zhang¹³, Yiyun Zhang¹⁴, Z. X. Zhang¹², Z. P. Zhang¹⁷, D. X. Zhao¹, J. W. Zhao¹, M. G. Zhao¹, P. P. Zhao¹, W. R. Zhao¹, Z. G. Zhao^{1h}, H. Q. Zheng¹², J. P. Zheng¹, Z. P. Zheng¹, L. Zhou¹, K. J. Zhu¹, Q. M. Zhu¹, Y. C. Zhu¹, Y. S. Zhu¹, Z. A. Zhu¹, B. A. Zhuang¹, X. A. Zhuang¹, B. S. Zou¹

(BES Collaboration)

¹ Institute of High Energy Physics, Beijing 100049, People's Republic of China

² China Center for Advanced Science and Technology (CCAST), Beijing 100080, People's Republic of China

³ Guangxi Normal University, Guilin 541004, People's Republic of China

⁴ Guangxi University, Nanning 530004, People's Republic of China

⁵ Henan Normal University, Xinxiang 453002, People's Republic of China

⁶ Huazhong Normal University, Wuhan 430079, People's Republic of China

⁷ Hunan University, Changsha 410082, People's Republic of China

⁸ Jinan University, Jinan 250022, People's Republic of China

⁹ Liaoning University, Shenyang 110036, People's Republic of China

¹⁰ Nanjing Normal University, Nanjing 210097, People's Republic of China

¹¹ Nankai University, Tianjin 300071, People's Republic of China

¹² Peking University, Beijing 100871, People's Republic of China

¹³ Shandong University, Jinan 250100, People's Republic of China

¹⁴ Sichuan University, Chengdu 610064, People's Republic of China

¹⁵ Tsinghua University, Beijing 100084, People's Republic of China

¹⁶ University of Hawaii, Honolulu, HI 96822, USA

¹⁷ University of Science and Technology of China, Hefei 230026, People's Republic of China

¹⁸ Wuhan University, Wuhan 430072, People's Republic of China

¹⁹ Zhejiang University, Hangzhou 310028, People's Republic of China

^a Current address: DESY, D-22607, Hamburg, Germany

^b Current address: Johns Hopkins University, Baltimore, MD 21218, USA

^c Current address: University of Oklahoma, Norman, Oklahoma 73019, USA

^d Current address: Universite Paris XI, LAL-Bat. 208- -BP34, 91898-ORSAY Cedex, France

^e Current address: Max-Planck-Institut fuer Physik, Foehringer Ring 6, 80805 Munich, Germany

^f Current address: University of Toronto, Toronto M5S 1A7, Canada

^g Current address: CERN, CH-1211 Geneva 23, Switzerland

^h Current address: University of Michigan, Ann Arbor, MI 48109, USA

(Dated: February 2, 2008)

Using 58 million J/ψ events collected with the Beijing Spectrometer (BESII) at the Beijing Electron-Positron Collider, the decays $J/\psi \rightarrow \gamma\phi\rho$ and $J/\psi \rightarrow \gamma\omega\rho$ are searched for, and upper limits on their branching fractions are reported at the 90% C. L. No clear structures are observed in the $\gamma\rho$, $\gamma\phi$, or $\rho\phi$ mass spectra for $J/\psi \rightarrow \gamma\phi\rho$ nor in the $\gamma\rho$, $\gamma\omega$, or $\rho\omega$ mass spectra for $J/\psi \rightarrow \gamma\omega\rho$.

I. INTRODUCTION

QCD predicts a rich spectrum of gg glueballs, ggq hybrids and $qq\bar{q}\bar{q}$ four quark states along with the ordinary $q\bar{q}$ mesons in the 1.0 to 2.5 GeV/ c^2 mass region. Radiative J/ψ decays provide an excellent laboratory to search for these states. Until now, no unique experimental signatures of such states have been found.

Systems of two vector particles have been intensively studied for signatures of gluonic bound states. Pseudoscalar (0^-) enhancements in $\rho\rho$, $\omega\omega$, and $\phi\phi$ final states have been seen in radiative J/ψ decays [1–7], and a scalar (0^+) enhancement near $\omega\phi$ threshold is observed from the doubly OZI suppressed decay of $J/\psi \rightarrow \gamma\omega\phi$ with mass $M = 1812_{26}^{+19} \pm 18$ MeV/ c^2 and width $\Gamma = 105 \pm 20 \pm 28$ MeV/ c^2 [8]. The radiative J/ψ decays $J/\psi \rightarrow \gamma\rho\phi$ and $J/\psi \rightarrow \gamma\rho\omega$ are OZI suppressed processes, and the measurements of these two decays and the search for possible resonant states in their decay products will provide useful information on two vector meson systems.

The double radiative channels $J/\psi \rightarrow \gamma X$, $X \rightarrow \gamma V$ ($V = \rho, \phi$ and ω) are studied to probe the quark content of the object X . The $\eta(1440)$ has been studied by the BES Collaboration through the double radiative channels $J/\psi \rightarrow \gamma(\gamma\rho)$ and $J/\psi \rightarrow \gamma(\gamma\phi)$ [9]. At one time, the $\eta(1440)$, after it was observed in J/ψ decay [10], was regarded as a glueball candidate. But this viewpoint changed when its radiative decay modes were observed. The $\eta(1440)$ is seen (at 1424 MeV/ c^2) by the BES Collaboration to decay strongly into $\gamma\rho$, not $\gamma\phi$. From this result, one cannot draw a definite conclusion on whether the $\eta(1440)$ is either a $q\bar{q}$ state or a glueball state. Therefore, further study is needed to clarify the situation. The process $J/\psi \rightarrow VX$, $X \rightarrow \gamma V$ also allows us to study X using the γV system.

In this letter, we report on the measurements of $J/\psi \rightarrow \gamma\rho\phi$ and $J/\psi \rightarrow \gamma\rho\omega$ decays and the search for possible structure in the γV and VV invariant mass spectra, using 58M J/ψ events collected with the Beijing Spectrometer (BESII) at the Beijing Electron-Positron Collider (BEPC) [11].

II. DETECTOR AND DATA ANALYSIS

BESII is a conventional solenoidal magnet detector that is described in detail in Refs. [11]. A 12-layer vertex chamber (VC) surrounding the beam pipe provides coordinate and trigger information. A forty-layer main drift chamber (MDC), located radially outside the VC, provides trajectory and energy loss (dE/dx) information for tracks over 85% of the total solid angle. The momentum resolution is $\sigma_p/p = 0.017\sqrt{1+p^2}$ (p in GeV/ c), and the dE/dx resolution for hadron tracks is $\sim 8\%$. An array of 48 scintillation counters surrounding the MDC measures

the time-of-flight (TOF) of tracks with a resolution of ~ 200 ps for hadrons. Radially outside the TOF system is a 12 radiation length, lead-gas barrel shower counter (BSC) which measures the energies of electrons and photons over $\sim 80\%$ of the total solid angle with an energy resolution of $\sigma_E/E = 22\%/\sqrt{E}$ (E in GeV). Outside of the solenoidal coil, which provides a 0.4 tesla magnetic field over the tracking volume, is an iron flux return that is instrumented with three double layers of counters that identify muons of momentum greater than 0.5 GeV/ c .

A. General selection criteria

All the charged tracks are reconstructed in the MDC, and the number of charged tracks is required to be four with net charge zero. Each track should (1) have a good track fit; (2) have $|\cos\theta| < 0.8$, where θ is the polar angle of the track measured by the MDC; (3) originate from the interaction region, $\sqrt{V_x^2 + V_y^2} < 2$ cm and $|V_z| < 20$ cm, where V_x , V_y , and V_z are the x, y, and z coordinates of the point of closest approach of the track to the beam axis; and (4) be identified as either a pion or a kaon. The particle identification (PID) is accomplished using the TOF information and the dE/dx information from the MDC [9]. For instance, a pion should have a higher particle PID confidence level than those for other hypotheses (kaon, proton).

A neutral cluster in the BSC is considered to be a photon candidate when its energy deposit in the BSC is greater than 30 MeV, the angle between the nearest charged track and the cluster is greater than 10° (to reject photons associated with the charged particles), the first hit appears in the first five layers of the BSC (about six radiation lengths of material), and the angle between the cluster development direction in the BSC and the photon emission direction is less than 25° . If the angle between two photons is less than 15° , and the invariant mass of these two photons is less than 60 MeV/ c^2 , the two photons are merged.

B. Analysis of $J/\psi \rightarrow \gamma\phi\rho$

For the channel $J/\psi \rightarrow \gamma\phi\rho$ ($\phi \rightarrow K^+K^-$, $\rho \rightarrow \pi^+\pi^-$), we require two pions, two kaons, and at least one photon with energy greater than 50 MeV. Next, the selected charged tracks and photon are fitted kinematically using energy and momentum conservation constraints (4C), looping over all photon candidates. The combination with the minimum χ^2 is selected, and the photon in this combination is taken as the radiative photon. Next, we require the energy of the radiative photon to be greater than 0.1 GeV and the fit χ^2 to be less than 8.0. The χ^2 requirement is determined by optimizing the

signal (S) to noise (B) ratio ($S/\sqrt{S+B}$), where $S+B$ is determined from data and S is determined from Monte Carlo (MC) simulation after event selection.

In order to suppress backgrounds from J/ψ two body decay channels with a ϕ , for example $J/\psi \rightarrow \phi\eta$ and $J/\psi \rightarrow \phi\eta'(958)$, the ϕ momentum is required to satisfy $P_\phi \leq 1.1$ GeV/ c . To select ϕ particles, the K^+K^- invariant mass is required to satisfy $|M_{K^+K^-} - M_\phi| \leq 0.01$ GeV/ c^2 .

The main expected background channels can be divided into the following five groups: (1) $J/\psi \rightarrow \phi\eta$, $\phi\eta'(958)$; (2) $J/\psi \rightarrow \omega KK$, ϕKK ($\phi \rightarrow \pi^+\pi^-\pi^0$); (3) $J/\psi \rightarrow \omega f_0(980)$ ($f_0(980) \rightarrow K^+K^-$); (4) $J/\psi \rightarrow \phi\pi\pi$, $\phi f_0(980)$; and (5) $J/\psi \rightarrow (\gamma)K^*(892)\bar{K}^*(892)$, $(\gamma, \pi^0)\pi^+\pi^-K^+K^-$. Since $J/\psi \rightarrow \pi^0\rho\phi$ is forbidden by C-parity conservation, it can be neglected in our background analysis. The $\pi^+\pi^-$ invariant mass distributions from all above possible background channels are smooth with no ρ peak according to MC simulations; therefore they will not affect the determination of the number of signal events.

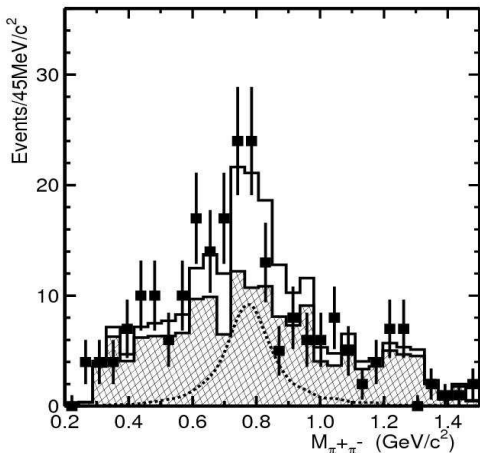


FIG. 1: The $\pi^+\pi^-$ invariant mass distribution. The square points with error bars are data, the shaded histogram is from the ϕ sideband events, the dotted curve is the signal shape from MC simulation, and the blank histogram is the fit.

The $\pi^+\pi^-$ invariant mass distribution for events that survive the selection criteria is shown in Fig. 1, and the $\pi^+\pi^-$ invariant mass distribution from ϕ sidebands ($1.05 < M_{K^+K^-} < 1.08$ GeV/ c^2 or $0.985 < M_{K^+K^-} < 0.992$ GeV/ c^2) scaled to the amount of background in the signal region is also shown as the shaded histogram.

By fitting the $\pi^+\pi^-$ invariant mass distribution with a ρ signal shape obtained from MC simulation and using the histogram from ϕ sideband events to describe the background shape, 43.2 ± 18.8 signal events are obtained, as shown in Fig. 1. The ρ signal statistical significance is estimated by comparing the likelihood values with and without the signal in the fit, and it is only about 2σ . The detection efficiency is $(3.33 \pm 0.04)\%$ from MC simulation.

Figures 2 (a) and (b) show the invariant mass distributions of $\gamma\rho$ and $\gamma\phi$; and Figs. 2 (c) and (d) show the

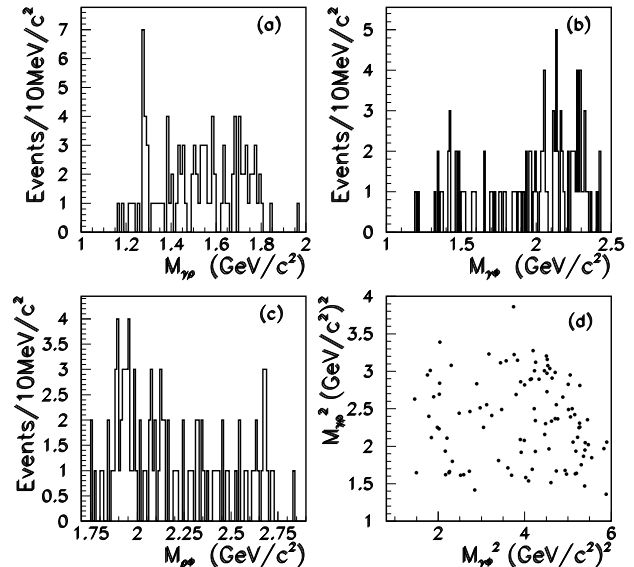


FIG. 2: (a) The $\gamma\rho$ invariant mass spectrum after ϕ selection ($|M_{K^+K^-} - M_\phi| \leq 0.01$ GeV/ c^2), (b) the $\gamma\phi$ invariant mass spectrum after ρ selection ($|M_{\pi^+\pi^-} - M_\rho| \leq 0.15$ GeV/ c^2), (c) the $\rho\phi$ invariant mass spectrum, and (d) the Dalitz plot of $M_{\gamma\phi}^2$ versus $M_{\gamma\rho}^2$.

$\rho\phi$ mass distribution and Dalitz plot of $M_{\gamma\phi}^2$ versus $M_{\gamma\rho}^2$ for $J/\psi \rightarrow \gamma\phi\rho$ candidates, where, the $\pi^+\pi^-$ invariant mass of the ρ candidates must satisfy $|M_{\pi^+\pi^-} - M_\rho| \leq 0.15$ GeV/ c^2 . No clear structure around 1440 MeV/ c^2 region is observed in the $M_{\gamma\rho}$ distribution. There may be some structures in the $\gamma\phi$ and $\rho\phi$ mass spectra, but because of the low statistics, it is difficult to determine whether they are real resonances or just statistical fluctuations.

The systematic errors, are evaluated with selected samples that are compared with MC simulations. In this analysis, the systematic errors on the branching fraction mainly come from the following sources:

(1). *Particle identification (PID)*. In Ref. [12], the PID efficiencies of pions and kaons are analyzed in detail. Here, two charged tracks are required to be identified as pions, and the other two are required to be kaons, so the systematic error from PID should be less than 4%.

(2). *MDC tracking and kinematic fit*. In order to study the systematic errors from the MDC tracking and kinematic fit, many distributions from data, including the wire efficiency and space resolution of hits in the MDC, are compared with those from MC simulations, using two different treatments of the wire resolution simulation. The difference between the two simulations is taken as the systematic error for the tracking [12]. In this paper, 13.5% is conservatively taken to be the systematic error from MDC tracking and kinematic fit.

(3). *Photon detection efficiency*. The photon detection

efficiency is studied using $J/\psi \rightarrow \rho^0 \pi^0$ in Ref. [12]. The results indicate that the systematic error is less than 2% for each photon.

(4). *Background uncertainty.* In order to determine the background uncertainty, several background assumptions were tried, including: (a) a fourth order polynomial function, (b) the background shape from MC simulations, and (c) the histogram from ϕ sideband events. The differences between the different fit results are taken as the systematic error, which is about 13.0%.

(5). *Intermediate decay branching fraction and the uncertainty of the number of J/ψ events.* The ϕ decay branching fraction (1.2%) from Ref. [13], and the uncertainty in the total number of J/ψ events (4.72%) are also considered as sources of the systematic error.

Adding all errors in quadrature, the total error is about 20.0%.

Finally the branching fraction is:

$$Br(J/\psi \rightarrow \gamma \phi \rho) = (4.5 \pm 2.0 \pm 0.9) \times 10^{-5},$$

where the first error is statistical and the second is the systematic. Since the statistical significance of the ρ signal is only 2σ , the upper limit (90% C.L.) is also determined by a Bayesian method [13]:

$$Br(J/\psi \rightarrow \gamma \phi \rho) < 8.8 \times 10^{-5}.$$

C. Analysis of $J/\psi \rightarrow \gamma \omega \rho$

For the channel $J/\psi \rightarrow \gamma \omega \rho$ ($\omega \rightarrow \pi^+ \pi^- \pi^0$, $\rho \rightarrow \pi^+ \pi^-$, $\pi^0 \rightarrow \gamma \gamma$), we require four pions and greater than two photons, where the energy of the photon candidates should be greater than 50 MeV. Next, the selected charged tracks and three photons are fitted using a 4C kinematic fit, looping over all photon candidates, under the hypothesis of $J/\psi \rightarrow 3\gamma 2(\pi^+ \pi^-)$. The combination with the minimum χ^2 is selected, and the χ^2 is required to be less than 9.0, which corresponds to the best signal-noise ratio. The two photons with invariant mass closest to the π^0 mass are regarded as being from π^0 decay, and the other is taken as the radiative photon. Finally, a 5C kinematic fit is made under the $J/\psi \rightarrow \gamma 2(\pi^+ \pi^-) \pi^0$ hypothesis with the invariant mass of the $\gamma \gamma$ pair associated with the π^0 being constrained to m_{π^0} . After the 5C kinematic fit, we require χ_{5C}^2 to be less than 9.0 and the energy of the radiative photon to be greater than 0.1 GeV.

The $\pi^+ \pi^-$ and $\pi^+ \pi^- \pi^0$ combinations for the ρ and ω candidates are selected from the minimum value of

$$\sqrt{\left(\frac{M_{\pi_1^+ \pi_2^-} - M_\rho}{\sigma_\rho}\right)^2 + \left(\frac{M_{\pi_3^+ \pi_4^- \pi^0} - M_\omega}{\sigma_\omega}\right)^2},$$

where σ_ρ and σ_ω are the widths (the mass resolutions are included) of ρ and ω , respectively, from MC simulations.

To select the ω candidates, we require $|M_{\pi_3^+ \pi_4^- \pi^0} - M_\omega| \leq 0.023 \text{ GeV}/c^2$.

In order to suppress the backgrounds from J/ψ two body decay channels with an ω , for example $J/\psi \rightarrow \omega \eta$ and $J/\psi \rightarrow \omega \eta'(958)$, the ω momentum must satisfy $P_\omega \leq 1.2 \text{ GeV}/c$. Similarly we also use $P_\rho \leq 1.1 \text{ GeV}/c$ to suppress the backgrounds from J/ψ two body decay channels with a ρ resonance.

The possible background channels of $J/\psi \rightarrow \gamma \omega \rho$ can be divided into the following four groups: (1) $J/\psi \rightarrow \omega \eta$, $\omega \eta'(958)$, $\omega \pi^+ \pi^-$, $\omega f_0(980)$, $\gamma \omega \omega$, $b_1(1235)^\pm \pi^\mp$; (2) $J/\psi \rightarrow a_2(1320) \rho$, $\rho \eta$, $\rho \eta'$, $\gamma \rho \rho$, $\gamma \eta_c$ ($\eta_c \rightarrow \rho \rho$); (3) $J/\psi \rightarrow 2(\pi^+ \pi^-) \pi^0$, $\gamma 2(\pi^+ \pi^-)$, $\gamma \eta \pi \pi$, $\gamma \eta'$; and (4) $J/\psi \rightarrow \gamma X$ ($X \rightarrow \eta \pi \pi$, $K^* \bar{K}^*$). Since $J/\psi \rightarrow \pi^0 \omega \rho$ is forbidden by C-parity conservation, it can be neglected in our background analysis. The contamination from all the above possible backgrounds after event selection is found to be very small according to MC simulation.

Figures 3 and 4 show $\pi^+ \pi^- \pi^0$ and $\pi^+ \pi^-$ invariant mass distributions and the $\pi^+ \pi^-$ mass distribution of ω sidebands ($0.6 < M_{\pi^+ \pi^- \pi^0} < 0.67 \text{ GeV}/c^2$ or $0.915 < M_{\pi^+ \pi^- \pi^0} < 0.95 \text{ GeV}/c^2$), scaled to the amount of background in the signal region and shown as the shaded histogram in Fig. 4. After subtracting the ω sideband events, we fit the $\pi^+ \pi^-$ invariant mass distribution to obtain the number of $J/\psi \rightarrow \gamma \omega \rho$ events.

Although the branching fraction of $\rho \rightarrow \pi^+ \pi^-$ ($\sim 100\%$) is about two orders of magnitude larger than that of $\omega \rightarrow \pi^+ \pi^-$ (1.7%), the interference between ρ and ω must be considered, and therefore, the fit function is expressed as [14]:

$$N(M_{\pi^+ \pi^-}) = L(M_{\pi^+ \pi^-}) + |A_\rho(M_{\pi^+ \pi^-}) + A_\omega(M_{\pi^+ \pi^-}) e^{i\varphi}|^2,$$

where L is a polynomial background term, φ is the relative phase angle between the two amplitudes, A_ρ and A_ω , which are represented by Breit-Wigner functions up to a numerical factor:

$$A_V(M_{\pi^+ \pi^-}) = \sqrt{N_V} F_{BW_V}(M_{\pi^+ \pi^-})(V \equiv \rho, \omega),$$

and the Breit-Wigner functions have an s-independent width:

$$F_{BW} = \frac{\Gamma M}{s - M^2 + iM\Gamma}.$$

Finally, the number of ρ events (181.3 ± 72.7), the number of ω events (76.6 ± 61.2), and the relative phase angle (39.4 ± 36.4) $^\circ$ are obtained; the fit is shown in Fig. 5. The statistical significance of the ρ signal is about 3.1σ , and the detection efficiency is about $(1.36 \pm 0.01)\%$ from MC simulation.

Figures 6 (a) and (b) show the invariant mass distributions of $\gamma \omega$ and $\gamma \rho$, and Figs. 6 (c) and (d) show the $\rho \omega$ mass distribution and Dalitz plot of $M_{\gamma \rho}^2$ versus $M_{\gamma \omega}^2$ for the $J/\psi \rightarrow \gamma \omega \rho$ candidates, where the ρ signal is selected using $|M_{\pi^+ \pi^-} - M_\rho| \leq 0.15 \text{ GeV}/c^2$. No clear structure around $1440 \text{ MeV}/c^2$ region is observed in the $M_{\gamma \rho}$ distribution. Although there is a hint of a possible structure

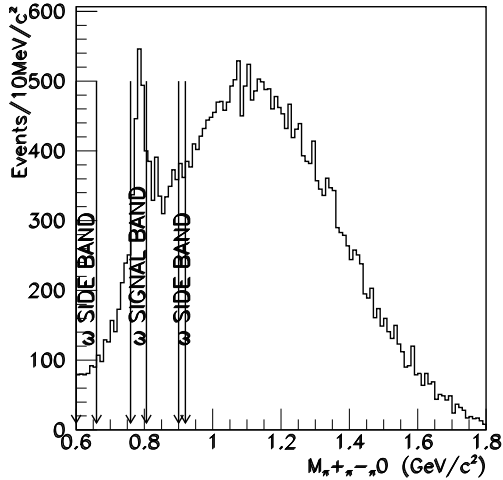


FIG. 3: The $\pi^+\pi^-\pi^0$ invariant mass spectrum. The ω signal and ω side band regions are indicated by arrows.

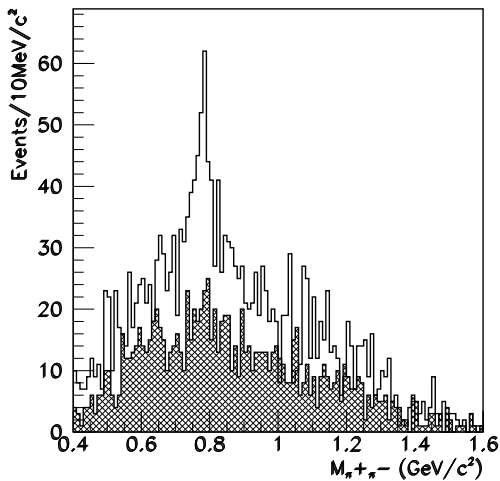


FIG. 4: The $\pi^+\pi^-$ invariant mass distribution. The shaded histogram is the distribution from ω sideband events which has been scaled to the amount of background in the signal region.

around $1700 \text{ MeV}/c^2$ in the $\rho\omega$ mass spectrum compared with the scaled $\rho\omega$ mass distribution from ρ and ω sideband events, it is difficult, because of the low statistics, to determine whether it is a real resonance or just due to a statistical fluctuation. Finally, only the branching fraction of $J/\psi \rightarrow \gamma\omega\rho$ is given.

Systematic errors in the $J/\psi \rightarrow \gamma\omega\rho$ branching fraction measurement are analyzed similarly as in the $J/\psi \rightarrow \gamma\phi\rho$ channel, which mainly come from particle identification (4%), the MDC tracking and the kinematic fit (11.5%), the photon detection efficiency (6%), the fitting procedures and different treatments of the backgrounds

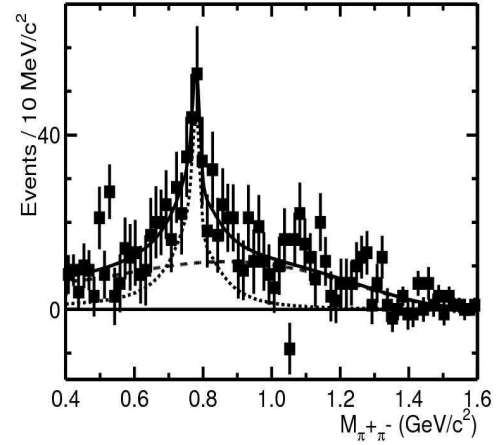


FIG. 5: The fit, described in the text, to the $\pi^+\pi^-$ invariant mass distribution. Here the squares with error bars are data, the dotted curve is the total signal from ρ and ω (the interference between them is also included), the dashed curve is the polynomial background, and the solid curve is the fit.

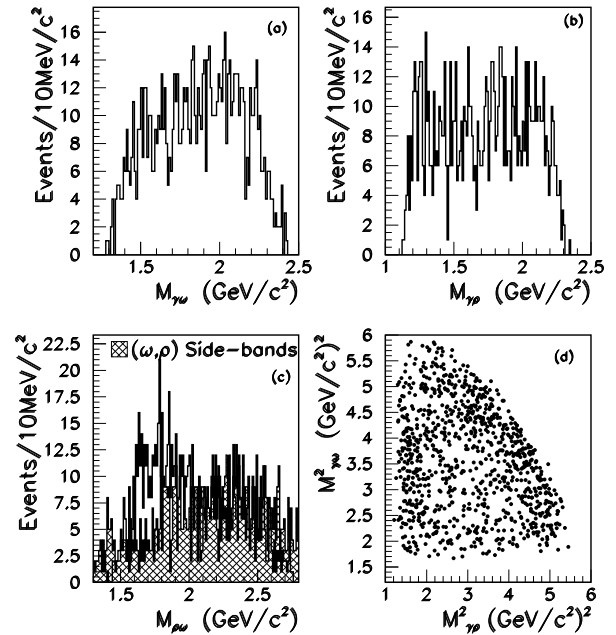


FIG. 6: (a) The $\gamma\omega$ invariant mass spectrum after ρ selection ($|M_{\pi^+\pi^-} - M_\rho| \leq 0.15 \text{ GeV}/c^2$), (b) the $\gamma\rho$ invariant mass spectrum after ω selection ($|M_{\pi^+\pi^-\pi^0} - M_\omega| \leq 0.023 \text{ GeV}/c^2$), (c) the $\rho\omega$ invariant mass spectrum (the shaded histogram is the scaled $\rho\omega$ mass spectrum of ρ and ω sidebands events), and (d) the Dalitz plot of $M_{\gamma\rho}^2$ versus $M_{\gamma\omega}^2$.

(21.6%), the total number of J/ψ events (4.72%), and the ω decay branching fraction (0.8%), taken from Ref. [13]. The total systematic error is 26.0%.

Finally, the branching fraction can be obtained:

$$Br(J/\psi \rightarrow \gamma\omega\rho) = (2.6 \pm 1.1 \pm 0.7) \times 10^{-4},$$

where the first error is statistical and the second is the

systematic. Since the statistical significance of the ρ signal is only 3.1σ , the upper limit (90% C.L.) is also estimated by a Bayesian method [13]:

$$Br(J/\psi \rightarrow \gamma\omega\rho) < 5.4 \times 10^{-4}.$$

III. CONCLUSION

Table I summarizes our results for the $J/\psi \rightarrow \gamma VV$ branching fractions; it also lists our $J/\psi \rightarrow \gamma\omega\omega$ branching fraction with one of ω decays to $\pi^+\pi^-$, which has a very small branching fraction (15.9%). Taking into consideration its large statistical error, this branching fraction is consistent with the value from Ref. [13].

As a check, the $J/\psi \rightarrow \gamma\omega\omega$ branching fraction was fixed at the value from Ref. [13] and the previous result from BES Collaboration [1], and the fit was redone to obtain the $J/\psi \rightarrow \gamma\omega\rho$ branching fraction. This branching fraction is not sensitive to that of $J/\psi \rightarrow \gamma\omega\omega$.

From our analysis of these two channels, we did not

observe any clear structures in either the VV or γV mass spectra.

IV. ACKNOWLEDGMENTS

The BES collaboration thanks the staff of BEPC and computing center for their hard efforts. This work is supported in part by the National Natural Science Foundation of China under contracts Nos. 10491300, 10225524, 10225525, 10425523, 10625524, 10521003, the Chinese Academy of Sciences under contract No. KJ 95T-03, the 100 Talents Program of CAS under Contract Nos. U-11, U-24, U-25, and the Knowledge Innovation Project of CAS under Contract Nos. U-602, U-34 (IHEP), the National Natural Science Foundation of China under Contract No. 10225522 (Tsinghua University), and the Department of Energy under Contract No. DE-FG02-04ER41291 (U. Hawaii).

-
- [1] BES Collaboration, M. Ablikim *et al.*, Phys. Rev. D **73**, 112007 (2006).
 - [2] MARK-III Collaboration, R. M. Baltrusaitis *et al.*, Phys. Rev. D **33**, 1222 (1986).
 - [3] D. L. Burke *et al.*, Phys. Rev. Lett. **49**, 632 (1982).
 - [4] MARK-III Collaboration, R. M. Baltrusaitis *et al.*, Phys. Rev. Lett. **55**, 1723 (1985).
 - [5] MARK-III Collaboration, Z. Bai *et al.*, Phys. Rev. Lett. **65**, 1309 (1990).
 - [6] DM2 Collaboration, D. Bisello *et al.*, Phys. Lett. B **241**, 617 (1990).
 - [7] DM2 Collaboration, D. Bisello *et al.*, Phys. Lett. B **179**, 294 (1986).
 - [8] BES Collaboration, M. Ablikim *et al.*, Phys. Rev. Lett. **96**, 162002 (2006).
 - [9] BES Collaboration, J. Z. Bai *et al.*, Phys. Lett. B **594**, 47 (2004).
 - [10] D. L. Scharre *et al.*, Phys. Lett. B **97**, 329 (1980).
 - [11] BES Collaboration, J. Z. Bai *et al.*, Nucl. Instr. Meth. Phys. Res. A **458**, 627 (2001); BES Collaboration, J. Z. Bai *et al.*, Nucl. Instr. Meth. Phys. Res. A **344**, 319 (1994).
 - [12] BES Collaboration, J. Z. Bai *et al.*, Phys. Rev. D **70**, 012005 (2004); BES Collaboration, M. Ablikim *et al.*, Nucl. Instr. Meth. Phys. Res. A **552**, 344 (2005); BES Collaboration, M. Ablikim *et al.*, Phys. Rev. D **71**, 032003 (2005); BES Collaboration, M. Ablikim *et al.*, Phys. Rev. D **73**, 052007 (2006).
 - [13] Particle Data Group, W.-M. Yao *et al.*, J. Phys. G **33**, 895 (2006).
 - [14] DM2 Collaboration, J. Jousset *et al.*, Phys. Rev. D **41**, 1389 (1990); MARK-III Collaboration, D. Coffman *et al.*, Phys. Rev. D **38**, 2695 (1988).

TABLE I: The branching fractions of $J/\psi \rightarrow \gamma VV$

Decay Mode	This Work	Ref. [13]	BESII [†]
$J/\psi \rightarrow \gamma\omega\rho$	$(2.6 \pm 1.1 \pm 0.7) \times 10^{-4}$ $(< 5.4 \times 10^{-4})$ (90% C.L.)		
$J/\psi \rightarrow \gamma\phi\rho$	$(4.5 \pm 2.0 \pm 0.9) \times 10^{-5}$ $(< 8.8 \times 10^{-5})$ (90% C.L.)		
$J/\psi \rightarrow \gamma\omega\omega$ one $\omega \rightarrow \pi^+\pi^-$	$(6.0 \pm 4.8 \pm 1.8) \times 10^{-3}$ $(< 1.7 \times 10^{-2})$ (90% C.L.)	$(1.59 \pm 0.33) \times 10^{-3}$	$(2.29 \pm 0.08) \times 10^{-3}$

[†] Result from $J/\psi \rightarrow \gamma\eta(1770) \rightarrow \gamma\omega\omega$ [1]